Slowly digestible properties of lotus seed starch - glycerine monostearin complexes formed by high pressure homogenization

Bingyan Chen, Xiangze Jia, Song Miao, Shaoxiao Zeng, Zebin Guo, Yi Zhang, Baodong Zheng

PII: S0308-8146(18)30063-3
DOI: https://doi.org/10.1016/j.foodchem.2018.01.054
Reference: FOCH 22243

To appear in: *Food Chemistry*

Received Date: 23 October 2017
Revised Date: 5 January 2018
Accepted Date: 6 January 2018

Please cite this article as: Chen, B., Jia, X., Miao, S., Zeng, S., Guo, Z., Zhang, Y., Zheng, B., Slowly digestible properties of lotus seed starch - glycerine monostearin complexes formed by high pressure homogenization, *Food Chemistry* (2018), doi: https://doi.org/10.1016/j.foodchem.2018.01.054

Slowly digestible properties of lotus seed starch - glycerine monostearin complexes formed by high pressure homogenization

Bingyan Chen [a,b,d], Xiangze Jia [a,b], Song Miao [c,a,d], Shaoxiao Zeng [a,b], Zebin Guo [a,b], Yi Zhang[a, b*], Baodong Zheng [a,b,d,*]

[a] *College of Food Science, Fujian Agriculture and Forestry University, Fuzhou, Fujian 350002, China*

[b] *Fujian Province Key Laboratory of Quality Science and Processing Technology in Special Starch, Fujian Agriculture and Forestry University, Fuzhou 350002, China*

[c] *Teagasc Food Research Centre, Moorepark, Fermoy, Co. Cork, Ireland*

[d] *China-Ireland international Cooperation Centre for Food Material Science and Structure Design, Fujian Agriculture and Forestry University, Fuzhou, Fujian 350002, China*

* Corresponding author

(B. Zheng), College of Food Science, Fujian Agriculture and Forestry University, No.15 Shangxiadian Road, Cangshan District, Fuzhou City, Fujian Province, China.

E-mail address: zbdfst@163.com

(Y. Zhang), College of Food Science, Fujian Agriculture and Forestry University, No.15 Shangxiadian Road, Cangshan District, Fuzhou City, Fujian Province, China.

E-mail address: zyifst@163.com

Abstract

Starch-lipid complexes were prepared using lotus seed starch (LS) and glycerin monostearate (GMS) via a high-pressure homogenization process, and the effect of high pressure homogenization (HPH) on the slow digestion properties of LS-GMS was investigated. The digestion profiles showed HPH treatment reduced the digestive rate of LS-GMS, and the extent of this change was dependent on homogenized pressure. Scanning electron microscopy displayed HPH treatment change the morphology of LS-GMS, with high pressure producing more compact block-shape structure to resist enzyme digestion. The results of Gel-permeation chromatography and Small-angle X-ray scattering revealed high homogenization pressure impacted molecular weight distribution and semi-crystalline region of complexes, resulting in the formation of new semi-crystalline with repeat unit distance of 16-18nm and molecular weight distribution of 2.50-2.80×10^5 Da, which displayed strong enzymatic resistance. Differential scanning calorimeter results revealed new semi-crystalline lamellar may originate from type-II complexes that exhibited a high transition temperature.

Keywords: Lotus seed starch; glycerin monostearate; high pressure homogenization; slowly digestion properties; fine structure

1. Introduction

Starch is stored as discrete semi-crystalline granules in higher plants, and it is the major energy source in most staple foods. Starch digestion consists of three main phases: granule swelling, substrate binding, and glucose releasing (Miao, Jiang, Cui, Zhang, & Jin, 2015). After starchy food is consumed, the digestive enzymes first diffuse into the hydrated solid food matrix, bind to the swollen starch substrates that are then digested by α-amylase to α-limit dextrin, and finally there is cleavage of both α-1,4 and α-1,6 glycosidic bonds by brush border enzymes into glucose (Brayer, et al., 2000). Its digestion rate and extent in the small intestine have a significant impact on human health and nutrition. According to Englyst et al (1992), starch is nutritionally classified into rapidly digestible starch (RDS), slowly digestible starch (SDS) and resistant starch (RS) depending on the rate and extent of its digestion. Most of the starch in human diets is digested rapidly in the small intestine. However, a variable proportion, known as SDS, can produce a slow and sustained release of glucose in the gastrointestinal tract with a low glycemic response, which further reduces the risk of developing type II diabetes, obesity, and cardiovascular disease (Nugent, 2005). Therefore, changing starch food quality to have a higher proportion of SDS, is of increasing interest to the food industry and consumers.

Many studies have been reported which focus on the production of SDS using physical and chemical methods. He, Liu, and Zhang (2008) showed that SDS products were successfully prepared using waxy rice starch, by octenyl succinic anhydride esterification and heat-moisture treatment. Xu and Zhang (2014) reported that starch

granules can be encapsulated by zein protein, which limits water accessibility and starch swelling, further leading to a dense packing of starch material with a high proportion of SDS. Tian et al. (2014) found that high hydrostatic pressure (HHP) treatment of gelatinized rice starch produced slower digestibility than heat treatment. The higher SDS percentage was mainly attributed to the higher ratio of imperfect crystallites produced by HHP treatment. Additionally, Jo et al. (2016) employed glycogen branching enzyme and amylosucrase to control branch density and length to increase the yield of SDS products. In general, the creation of SDS is supported by different mechanistic paths, the slow digestion property being related to the supra-molecular semi-crystalline structure of amylopectin, which determines the possible changes to its physical state after starch gelatinization (Zhang, Ao, & Hamaker, 2006).

Recently, it has been widely accepted that amylose changes from a coil to a helix structure and forms an inclusion complex with polar lipids. This conformational ordering further promotes aggregation of helices, resulting in a partially crystalline structure that can decrease its susceptibility to amylase. Gelders et al. (2005) reported that hydrolysis of these complexes is influenced by amylose chain length, and that resistance to enzyme and acid hydrolysis increased with an increasing degree of polymerization. This has been confirmed by Putseys, Derde, Lamberts, Ostman, Björck, and Delcour (2010) who attributed this to the low solubility of the complexes and the steric hindrance they exert. However, other studies have different views that the digestion rate of starch complexes is only determined by the complex index (CI),

as complexes with low CI index were still hydrolyzed fully at high temperature (Kawai, Takato, Sasaki, & Kajiwara, 2012). Zhang et al. (2012) also reported a novel slow digestion starch made by debranched high-amylose starch complexed with lauric acid. Lipid properties also influence the digestibility of amylose-lipid complexes, and the extent of change depends on lipid chain lengths and degree of unsaturation; the longer the fatty acid chain, the greater the stability, and the lower the digestive rate of amylose-lipid complexes (Ai, Hasjim, & Jane, 2013). As yet there have been no studies of molecular structural changes during digestion of starch complexes.

Lotus (*Nelumbo nucifera Gaertn*), an aquatic plant from family Nelumbonaceae, is an important economic plant which is widely cultivated in China, Korea, Japan, Indian and Australia (Rai, Wahile, Mukherjee, Saha, & Mukherjee, 2006). Lotus seed is rich in starch, aroma, and minerals, which is used in the production of traditional confectionery products and food additives. However, lotus seed products have limited edible potential due to their rapid digestive properties and high glycemic response after consumption (Zeng et al., 2016). Thus, increasing the SDS content of lotus seed products is important for improving their acceptability to consumers. In our previous study, starch-lipid complexes prepared by lotus seed starch (LS) and glycerin monostearin (GMS) using high pressure homogenization (HPH), exhibited strong V-type crystal structure and high thermal stability (Chen, Zeng, Zeng, Guo, Zhang, & Zheng, 2017). We speculated these complexes may have increased enzyme hydrolysis resistance due to their high crystallinity. The lower digestibility rates suggest these starch complexes may be suited to the diets of obesity and diabetic patients. To date,

there is limited information on the effect of HPH treatment on the digestion properties of starch complexes. In addition, understanding the change to starch complexes during digestion would be helpful to form the basis for further investigation into the digestive behavior of starch-lipid complex.

The present study investigates the effect of HPH on the digestion properties of these complexes, exploring the evolution of molecular structure during the digestion process, and clarifying the relationship between molecular structure and slow digestion of these complexes. The digestibility was determined by first-order enzyme kinetic studies. The change in morphology and molecular structure was characterized by field emission electron microscopy (FESEM), gel-permeation chromatography (GPC), small angle X-ray scattering (SAXS) and differential scanning calorimetry (DSC).

2. Materials and methods

2.1. Materials

LS with an amylose/amylopectin ratio of 45/55 was obtained from Green Field Food Co., Ltd. (Fujian, China). The raw starch was defatted by ethanol washing and was dried in an air oven at 40 ± 1°C for 16 h. GMS with a hydrophilic–lipophilic balance of 3.8 was obtained from TNJ Chemical Industry Co., Ltd., China. α-Amylase from porcine pancreas, ≥50 units/mg protein, was purchased form Sigma-Aldrich Co Ltd., USA. Amyloglucosidase from *Aspergillus niger*, ≥260 unit/mL was from Sigma-Aldrich Co Ltd., Pullulan standards for SEC analysis were from Polymer Standards Service (PSS) GmbH, Germany, and cover the molecular weight range

from 342 to 2.35×10^6 Da. All other chemical reagents used in this study were of analytical grade.

2.2 Formation of the complexes by high-pressure homogenization

GMS (1.25 g, 5%, w/w, dry starch base) was dissolved in 50% ethanol solution and added to the defatted starch slurry (25 g, 5%, w/w). The mixtures were heated in a water bath at 90°C with vigorous stirring for 15 min, and then cooled to 60 °C. The mixture slurries (LS-GMS) were homogenized using a laboratory-scale high-pressure homogenizer (GYB 40-10S; Donghua Technology Co., Ltd., Shanghai, China) at 50 and 100 MPa for five passes. Approximately 500 mL of the starch suspensions were obtained at each pressure level. After high-pressure treatment, the homogenized samples were incubated at 25°C for 12 h. Samples were collected by centrifugation (4500×g, 10 min) and washed twice with a 50% ethanol mixture to remove any uncomplexed GMS. The final precipitates (LS-GMS-50 and LS-GMS-100) were freeze-dried and ground with a laboratory-scale grinder until able to pass through a 100-mesh sieve. As a control, a sample without GMS was also prepared.

2.3 In-vitro digestibility

The in vitro starch digestion was measured following a modified procedure according to the method of Zeng et al. (2016). Starch samples (300 mg, dry basis) were were dispersed with 5 mL of distilled water, and the cooked at 100°C for 10 min After cooling to 37°C in a water bath, they dispersed with 20 mL enzyme solution (0.1M sodium phosphate buffer, pH 6.5, 0.01%NaN_3, 2.5mM $CaCl_2$, 1500U α-amylase) in 50 mL screw-capped tubes. The reaction solution was shaken

(100rpm/min) and incubated at 37°C in a water bath, with 2 mL aliquots removed at a range of times and boiled to terminate the reaction. The digested starch suspensions were then added to 5 mL sodium acetate buffer solution (0.4M, pH 4.6), followed by addition of 1 mL amyloglucosidase (≥260 unit/mL), then the mixture was incubated at 50°C in a water bath for 45 min. The glucose content in the supernatant was measured using the 3,5-dinitrosalicylic acid (DNS) method. The starch residues at each time point (30, 60, 90, 120, 150, 180 min) were collected for structure analysis. The percentage of hydrolysed sample was calculated by multiplying the glucose content by a factor of 0.9. The values of RDS, SDS and RS fractions in each sample were obtained by the following equations:

$$RDS\ (\%) = [(G_{20} - FG)/TS] \times 0.9 \times 100$$

$$SDS\ (\%) = [(G_{120} - G_{20})/TS] \times 0.9 \times 100$$

$$RS\ (\%) = [(TS\text{-}G_{120})/TS] \times 0.9 \times 100$$

where, G20 and G120 are the amounts of glucose released within 20 and 120 min of hydrolysis, respectively, FG is the amount of free glucose in starch and TS is total starch weight.

2.4 Fitting to first-order kinetics

Digestibility curves were then fitted to a first-order equation (Eq.(1)), which in integrated form is:

$$C_t = C_\infty \left(1\text{-}e^{-kt}\right) \qquad (1)$$

C_t is the percentage of starch digested at time t (min), C_∞ is the estimated percentage of starch digested by the end of reaction time and k (min^{-1}) is the starch digestion rate coefficient, which was measured using a logarithm-of-slope (LOS)

analysis described in detail elsewhere (Edwards, Warren, Milligan, Butterworth, & Ellis, 2014) through a transformed equation:

$$\ln\left(dC_t/d_t\right) = \ln C_\infty k\text{-}kt \qquad (2)$$

The derivative dC_t/dt is obtained using second-order finite difference. From Eq (2), a plot of the logarithm of this derivative against time yields C_∞ and k, if this plot is linear.

2.5 Field emission electron microscopy

To analyze the morphology of starch samples before and after digestion, SEM graphs of starch residues were obtained with a field emission scanning electron microscope (JSM-6360LV, JEOL, Tokyo, Japan) in low vacuum mode at an accelerating voltage of 20 keV.

2.6 Gel-permeation chromatography (GPC) analysis

Gel-permeation chromatography (GPC) is a technique for separating molecules based on molecular hydrodynamic radius, R_h. The GPC analysis of starch residue was performed following the method of Man et al. (2014). Starch residues (12.5 mg) were dissolved in 20.0 mL of DMSO-0.5% (w/w) LiBr solution, stirred with a magnetic stirrer at 80^{o}C in a water bath overnight; the sample solutions were then centrifuged at 10000×g for 5 min. An aliquot of the supernatant (300 μL) was prepared for GPC analysis after passing through a 0.22μm nylon filter. The weight distribution, $logM_w$, of starch residues was characterized using an Agilent 1260 series (Agilent Technologies, USA) with a refractive index detector (Optilab T-rEX, WYATT Corp., USA). A GRAM pre-column, GRAM 100 and GRAM 3000 columns (PSS. Mainz,

Germany) were used with DMSO/LiBr eluent at 0.35 mL/min.

2.7 Small-angle X-ray scattering (SAXS)

Starch residues were dispersed in an excess of distilled water to form 40% starch slurry. SAXS measurement of starch suspensions was performed according to the method of Qiao et al. (2016) with some modifications. The X-ray source was a copper rotating anode (0.1 mm filament) operating at 50 kv and 30 W, fitted with cross coupled Göbel mirrors, resulting in Cu Ka radiation wavelength of 1.5418 Å. Scattering was detected in the q range of 0.007~0.23Å^{-1} for SAXS. SAXS data were analyzed using scatter brain software, and The Bragg spacing d was calculated from the position of the peak q_o) according to $d=2\pi/q_o$, Where $q=4\pi sin\theta/\lambda$ (where θ is the scattering angle and λ is the X-ray wavelength).

2.8 SAXS analysis

SAXS data from semi-crystalline structures can be analyzed by the one-dimensional linear correlation function L(r) which is derived from the Fourier transformation of the scattering curve using Eq.(4) and Eq.(5):

$$L(r)=\frac{\int_{\infty}^{0} I(q)q^2\cos(qr)dq}{Q} \quad (4)$$

The scattering invariant, Q, is defined as

$$Q=\int_0^{\infty} I(q)q^2dq \quad (5)$$

where I(q) is scattering intensity; r is the direction along the lamellar stack; the lamellar repeat distance (d) is the value of r at the second maximum of *L(r)*. The average thickness of the amorphous lamellae is expressed as d_a, which can be acquired by solution of the linear region and the flat *L(r)* minimum; Thus, d_c, the

average thickness of crystalline lamellae can be calculated by $d_c = d - d_a$.

2.9 Different scanning calorimetry (DSC)

The thermal behavior of starch residues was measured using a differential scanning calorimeter (DSC-200FC, NETZSCH, Selb, Germany) with nitrogen gas purge. A high pressure stainless pan with a gold-plated copper seal was used to run the test. Starch residues (3mg) were mixed with 10 μL of deionized water and hermetically sealed in a stainless steel pan, which were than kept at 25°C for 12h to achieve homogeneous samples. The samples were scanned between 25-180°C at a rate of 10°C/min. Calculated values for initial gelatin temperature (T_o) and enthalpy (ΔH) were recorded.

2.10 Data analysis

Graphs were constructed using Origin Pro 8.5. The data reported in all the tables are mean values with standard deviations. Analysis of variance (ANOVA) using LSD's test ($p < 0.05$) was evaluated using the DPS 9.05 Statistical Software Program (Science Press, Beijing, China).

3. Result and discussion

3.1 Starch digestion profiles

Fig.1 shows the typical digestion curves of LS and LS-GMS at different homogenization pressures. LS exhibited a high enzyme hydrolysis content, and a rapid hydrolysis rate was observed up to 30 min; when the enzyme hydrolysis curve reached a plateau, the starch hydrolysis content was 85.79%. LS appeared to be weakly resistant to enzymatic digestion, due to the higher degree of swelling and

partial disruption of starch amorphous structure in the heating process, resulting in an increased susceptibility of starch chains to digestive enzymes. The hydrolysis content of LS increased with increasing homogenized pressure. Similar results have been observed in previous studies (Stolt, Oinonen, & Autio, 2000), which indicated that high shear force can disrupt the integrity of starch granules and increase the interaction between the starch chains and the enzyme. Compared with LS, the hydrolysis content of LS-GMS declined to a great degree. The LS-GMS displayed a final value of 79.36%, 6.43% lower than LS, and the time to reach a plateau was extended. The variation of digestion patterns was consistent with Wang, Wang, Yu, and Wang (2016), who reported that complex formation contributed to the decrease in the extent of digestion by inhibiting the swelling of starch granules. Following the HPH treatment, LS-GMS showed an obvious notable decrease in its hydrolysis content. When homogenization pressure was raised to 100MPa, LS-GMS-100 showed a lower hydrolysis content than that of LS-GMS, indicating that HPH treatment increased enzymatic resistance of starch complexes. The extent of this change was dependent on the level of homogenization pressure.

A standard first-order rate equation can be used to investigate the kinetics of starch sample digestion (Zhang, Dhital, & Gidley, 2013). The fitting of first-order kinetics to starch digestions is shown in Fig. 1, and the digestion rate coefficients are presented in Table 1A. It is clear that all starch samples closely followed first-order behavior according to the R value (0.993-0.996) during digestion, indicating that the LOS model was capable of describing the starch digestion process accurately. LS and

LS-GMS had similar LOS plots in their digestion patterns, the latter having a lower k value. This means that both had a similar starch fraction that could be digested in the first phase, differing in their digestion rate, only. It is worth noting that the LOS plot of LS-GMS-100 retained two linear phases (dual-phase digestion); the first phase being similar to that of LS-100, having a higher digestion rate than the second ($k_1 > k_2$). The dual-phase digestion for LS-GMS-100 could be attributed to a change in the large-scale structure of the starch granules. As we reported before (Chen, Zeng, Zeng, Guo, Zhang, & Zheng, 2017), the crystalline structure of starch granules is damaged by strong mechanical forces, accompanied by the formation of a more compact complex crystalline form. Hence, it is proposed that the rapid digestion in the first phase mainly occurred to the amorphous residues, which originated in the disruption of starch granules at high pressure and shearing, whereas the more compact complexed fractions were less susceptible to the enzyme, resulting in their slower hydrolysis in the second phase. This finding was consistent with a previous study (Meng, Ma, Sun, Wang, & Liu, 2014), which reported that HPH treatment could significantly influence digestibility of corn starch complexes, with more highly crystalline complexes having lower digestibility.

The change in nutritional starch fractions is shown in Table 1A. The RDS, SDS and RS content in LS were 76.65%, 8.64%, 14.21%, respectively. The RDS content of LS increased with increasing homogenization pressure. In contrast for LS-GMS, the RDS fraction decreased significantly along with increased SDS content. When the homogenization pressure was raised to 100MPa, LS-GMS-100 showed the lowest

RDS content (39.17%) and highest SDS content (33.21%). The change in starch nutritional fractions further indicated that high homogenization pressure had a significant impact on the slowly digestible properties of starch complexes.

3.2 Change in granules morphology

The morphology changes of starch samples before and after digestion are shown in Fig.2. It is known (Zhang, Zeng, Wang, Zeng, & Zheng, 2014), that LS granules are oval and have a smooth and compact surface. The appearance of LS-50 became rough with shape distortion, but the granule morphology is not completely damaged and some intact granules can still be observed in the SEM image. When homogenization pressure reached 100MPa, the shape of the starch granules degraded markedly and they eventually disintegrated into amorphous structures. These results indicate that HPH treatment disrupted LS granules semi-crystalline structure. Furthermore, the LS granules lost their distinct shape after 180 min of digestion and a sheet-like structure was observed in the SEM image. This result is consistent with the result of starch digestion profiles, which showed an increase in the rapidly digestible properties of LS granules. When GMS was added to the starch system, LS granules adopted a different morphology. Some irregularly-shaped fragments were apparent on the surface of swollen starch granules, in agreement with observation reported by Chang, He, and Huang (2013), who attributed these crystal fragments to the presence of leached amylose, which readily interacted with available GMS to form helical complexes. The shape of LS-GMS granules was very different from that of LS after 180 min of digestion, still exhibiting an oval shape, with some granules having pits

and deformation. A similar result was also found in the SEM image of LS-GMS-50, consistent with starch complexes having a lower extent of digestion. It is notable that elevating the pressure to 100MPa destroyed all granule structure and the SEM image showed the formation of a large number of compact crystalline fragments in LS-GMS-100. The morphology of these complexes was not significantly changed after 180 min of digestion, and only a few holes appearing on the surface of crystalline fragments. These results suggest that high homogenization pressure has the capacity to induce changes in the morphology of complexes, further increasing their slowly digestible properties.

3.3 Change in molecule weight distribution

The molecular structure variation of starch chains during digestion, as determined by GPC, is shown in Fig. 3. LS exhibited a type single peak (Peak I) at high molecular weight distribution (6.07-6.98×10^6 Da), which was attributed to the high branched structure of amylopectin. The proportion of peak I in LS decreased rapidly during digestion, with a low molecular weight distribution (3.66-4.45×10^4 Da) appearing after 90 min of digestion. With further enzymatic hydrolysis, the proportion of low molecular weight distribution increased gradually, indicating that highly branched crystalline structure of the starch granules was somewhat hydrolysed by the digestive enzymes. Following HPH treatment, LS-50 showed no obvious difference in molecular weight distribution compared with LS. However, a typical trimodal distribution of low, middle, and high molecular weight peaks, designated peak 1 (8.21-9.49×10^6 Da), peak 2 (4.21-7.49×10^5 Da) and peak 3 (2.76-5.28×10^4 Da)

respectively, is observed in LS-100. The formation of low and middle molecular weight fractions in LS-100 can be attributed to the degradation of starch chains under high shear and pressure. This result was in agreement with previous study, which showed high pressure homogenization exhibited a strong impact on polymer charge and molar mass of starch (Villay, Filippis, Picton, Cerf, Vital, & Michaud, 2012). LS-100 exhibited a rapid transition from high and middle molecular weight fractions to low molecular weight fractions during digestion. When GMS was added into starch system, LS-GMS still included a single molecular weight peak ($6.62\text{-}6.87\times10^{6}$ Da). However, the change in molecular weight of LS-GMS was less than that of LS during digestion, and a large amount of middle molecular weight fragments ($5.07\text{-}5.27\times10^{5}$ Da) was observed after 180 min of digestion. This result was in agreement with Abhari et al. (2013), who indicated that enzyme penetration is hampered in the presence of amylose-inclusion complexes and result in reduced hydrolysis of the starch chain. Similar result was also found in that of LS-GMS-50. However, this process is different from the slowly hydrolysis mechanism of starch-tea polyphenols, which extended postprandial glycemic response via decreasing activity of mucosal α-glucosidase (Peng, Xue, Leng, Yang, Zhang, & Hamker, 2015). When the LS-GMS system was subjected to 100MPa, no obvious changes in the proportion of middle molecular weight ($2.50\text{-}2.80\times10^{5}$ Da) were observed during digestion. LS-GMS-100 showed that the high molecular weight fraction was hydrolysed into low molecular weight fraction during digestion. These results indicated that the middle molecular weight starch fraction can complex with GMS at high homogenization pressure and

these complexes displayed a significant enzymatic resistance during digestion.

3.4 Change in lamellar structure

The one-dimensional (1D) SAXS pattern of LS and LS-GMS at different homogenization pressures are shown in Fig.4A. It can be seen that the scattering intensity at low *q* values increased with increasing enzyme digestion time in all samples, which could result from the changes in the semi-crystalline region and the amorphous regions at the nano scale (Zhang, Li, Liu, Xie, & Chen, 2013). According to the paracrystalline model (Cameron & Donald, 1993), scattering peak intensity is positively correlated with the electron density difference $\Delta\rho$ (ρ_c - ρ_a) between the amorphous region (ρ_a) and semi-crystalline region (ρ_c). This supports the suggestion that the digestive enzyme disrupted more effectively the amorphous region rather than the semi-crystalline region in all samples. Apart from the increased scattering intensity of complexes at low *q* values, the scattering peak is influenced significantly by HPH treatment. For LS, starch granules have a unique semi-crystalline multi-scale structure with concentric layers of amorphous and crystalline lamellae radiating from the hilum (Zhu, 2017). Thus, a typical scattering peak (0.06-0.07$Å^{-1}$) was observed in the scattering pattern, indicating a 9~10 nm repeated semi-crystalline region according to Bragg's law $D=2\pi/q$ (Cai, Cai, Man, Yang, Zhang, & Wei, 2014; Cameron & Donald, 1992). The scattering peak at q of 0.06-0.07 $Å^{-1}$ almost disappeared entirely following 90 min of digestion, indicating the rapid disruption of the semi-crystalline region of LS during digestion. When GMS was added into the starch system, LS-GMS displayed a similar scattering peak at q of 0.06-0.07 $Å^{-1}$, and

the peak reduced slowly during digestion. This result suggested that complex formation had no obvious impact on the semi-crystalline structure of LS but did slow down the hydrolysis rate of the semi-crystalline region. Similar results were also found in LS-GMS treated at 50MPa. Moreover, when the homogenization pressure was raised to 100MPa, some distinct differences were observed in the SAXS patterns of LS-GMS-100. The scattering peak at q of 0.06-0.07$Å^{-1}$ disappeared, and LS-GMS-100 displayed a new scattering peak (0.034-0.040$Å^{-1}$), which showed no obvious change during the digestion process. This result was attributed to the fact that a large number of short linear starch chains interacted with GMS at high pressure, and these complexes helices further stack parallel into a V_H-type crystal structure (Goderis, Putseys, Gommes, Bosmans, & Delcour, 2014).

To clarify how the thickness of the semi-crystalline region evolved under enzymatic digestion, the average thicknesses of semi-crystalline (d), crystalline (d_c) and amorphous (d_a) lamellae were obtained using the Flourier transformation linear correlation function (Eq.(4) and Eq.(5)), and summarized in Fig.4B. For LS and LS-50, it can be seen that the crystalline lamellae were transformed to amorphous lamellae and the electron density of the semi-crystalline region decreased during digestion. LS-GMS exhibited the same trend in the change of semi-crystalline region compared with LS, but the electron density of the semi-crystalline region decreased more slowly. This result is in agreement with the SAXS patterns, further confirming that complexes can decrease the digestion rate of semi-crystalline regions of the starch granule. In contrast, the change in semi-crystalline region of complexes, which were

treated by HPH, was markedly different during digestion. The electron density of the semi-crystalline region of LS-GMS-100 was not affected significantly by the digestive enzyme, suggesting that high homogenization pressure (100MPa) has the capacity to generate more stable crystalline starch complexes with a repeat unit distance of 16-18nm, which contributed to their greater resistance to enzymatic digestion.

3.5 Thermal behaviors

To investigate the correlation between molecular arrangement and semi-crystalline structure during digestion, the thermal properties of LS and its complexes before and after enzyme hydrolysis were analysed (Table 1B). The initial gelatin temperature (T_o) and enthalpy change (ΔH) of LS decreased with increasing homogenization pressure, and reached their lowest values at 100MPa. No obvious enthalpy changes were observed in LS-100 after 60 min of digestion. These results confirmed that HPH treatment could disrupt the semi-crystalline structure of the starch granule, and further decrease the resistance of the semi-crystalline region to digestive enzymes. LS-GMS exhibited higher T_o and ΔH than that of LS, and LS-GMS also showed a smaller decrease in ΔH during digestion. This result was mainly attributed to the formation of type-I complexes, which not only prolong the dissociation of semi-crystalline structures, but also increase their enzymatic resistance. The thermal properties of LS-GMS were significantly changed by HPH treatment. LS-GMS-100 exhibited typical type-II complex characteristics with higher gelation temperature (T_o=108^{o}C) and enthalpy change (ΔH=3.54J/g). Type-II complexes have

a higher transition temperature than type-I complexes due to their compact crystalline region (Karkalas, Ma, Morrison, & Pethrick, 1995). Additionally, it can be seen that the enthalpy change (ΔH) of LS-GMS-100 was not impacted significantly by the digestive enzyme, and exhibited a slowest decrease during digestion. According to Garcia et al. (2016), amylose quantities and chain length directly influence complex formation and stability. Therefore, it was thought that the strong enzymatic resistance of LS-GMS-100 may be attributed to a large number of shorter linear starch chains, originating from the degradation of amylopectin under HPH treatment, thus providing greater stability to V-type complexes.

3.5 The relationship between the structure of starch complexes and slow digestive properties

The digestion properties of starch are related to the physical state of its crystalline region. Raw starch has a high proportion of SDS material as measured by the *in-vitro* Englyst method, and the slow digestion properties can be ascribed to 'inside-out' and 'exo-pitting' enzymatic hydrolysis patterns respectively, according to the different starch crystal forms (A-type or B-type) (Zhang & Hamaker, 2009). Generally, gelatinized starch granules are thought to have a high digestive rate, due to the disruption of amorphous regions of the granule and subsequent hydration, leading to a swelling of the ordered structure making them more readily available for amylase-catalyzed hydrolysis. Several studies have shown that starch inclusion complexes significantly reduced starch digestion rate, and the postprandial rise in blood glucose (Putseys, Lamberts, & Delcour, 2010; Zhang & Hamaker, 2009). In our

study, the slowly digestible behavior of complexes was clearly improved by HPH treatment. Changes in semi-crystalline structure were considered to be responsible for the changes in this behavior. For LS-GMS, complex formation had no obvious impact on the semi-crystalline region and the molecular weight distribution of the starch granule. However, leached amylose, which was mainly derived from the swelling of the granule exterior during heating, may immediately complex with GMS at the starch granule surface due to the strong hydrophobic interaction between them. This result is supported by SEM images (Fig.2). These complexes restrict the further swelling and solubility of starch granules and may act as a contiguous barrier layer to enzyme-substrate binding, further slowing down hydrolysis of semi-crystalline and amorphous regions, and resulting in the production of slowly digestible properties, as shown in Fig. 5A. The amorphous region of the complexes was more susceptible to hydrolysis, a finding supported by SAXS analysis, and this is likely to be due to the amorphous region lacking amylose after complex formation, making the glucan chains more mobile.

High homogenization pressure (100MPa) can markedly disrupt the semi-crystalline structure of starch granules, and change the molecule weight distribution of starch chains in a matrix. When the shorter starch chain complexed with GMS, high homogenization pressure facilitated the formation of more stable semi-crystalline lamellae, with a repeat unit distance of 16-18nm and molecular weight distribution of 2.50-2.80×10^5 Da, as shown in Fig.5B. This was supported by SAXS and GPC studies, which showed these complexes to have a greater enzymatic

resistance during digestion. This portion of the complexes (LS-GMS-100) was further determined to have a higher transition temperature (T_o=108°C) and enthalpy change (ΔH=3.54J/g), ascribed to type-II complexes. This result was also in agreement with previous studies (Gelders, Duyck, Goesaert, & Delcour, 2005; Tufvesson, Wahlgren, & Eliasson, 2003), indicating that crystalline amylose-lipid complexes (so-called type-II) are more enzyme resistant than their amorphous counterparts (so-called type-I).

4. Conclusion

The present work investigated the effect of HPH treatment on the slow digestion properties of LS-GMS. In general, slow digestion properties of LS-GMS could be improved significantly by HPH treatment, and the extent was dependent on homogenized pressure. High homogenization pressure (100MPa) could disrupt the semi-crystalline structure of starch granules and strengthen the interactions between LS and GMS, resulting in the change of complexes morphology and the formation of a new semi-crystalline structure, with a repeat unit distance of 16-18nm and molecular weight distribution of 2.50-2.80×10^5 Da. These were consistent with type-II complexes and displayed strong enzymatic resistance during digestion. HPH technology may be an effective way to increase the SDS content of starch complexes.

Acknowledgments

This study was financially supported by the National Natural Science Fundation of China (No. 31501485) and the Scientific and Technological Innovation Team Support Plan of Institution of Higher Learning in Fujian Province (Grant No.

[2012]03). The study was also supported by Doctoral Student Cooperation Research Project of Fujian Agriculture and Forestry University of China (Grant No. 324-112110075)

Reference

Ahmadi-Abhari, S., Woortman, A. J. J., Hamer, R. J., Oudhuis, A. A. C. M., & Loos, K. (2013). Influence of lysophosphatidylcholine on the gelation of diluted wheat starch suspensions. *Carbohydrate Polymers, 93*(1), 224-231.

Ai, Y., Hasjim, J., & Jane, J. L. (2013). Effects of lipids on enzymatic hydrolysis and physical properties of starch. *Carbohydrate Polymers, 92*(1), 120-127.

Cai, J., Cai, C., Man, J., Yang, Y., Zhang, F., & Wei, C. (2014). Crystalline and structural properties of acid-modified lotus rhizome C-type starch. *Carbohydrate Polymers, 102*(1), 799-807.

Cameron, R., & Donald, A. (1992). Small-angle X-ray scattering study of the annealing and gelatinization of starch. *Polymer, 33*(12), 2628-2635.

Cameron, R. E., & Donald, A. M. (1993). A small-angle x-ray scattering study of starch gelatinization in excess and limiting water. *Journal of Polymer Science Part B Polymer Physics, 31*(31), 1197-1203.

Chang, F., He, X., & Huang, Q. (2013). Effect of lauric acid on the V-amylose complex distribution and properties of swelled normal cornstarch granules. *Journal of Cereal Science, 58*(1), 89-95.

Chen, B., Zeng, S., Zeng, H., Guo, Z., Zhang, Y., & Zheng, B. (2017). Properties of lotus seed starch - glycerin monostearin complexes formed by high pressure homogenization. *Food Chemistry, 226*(1), 119-127.

Edwards, C. H., Warren, F. J., Milligan, P. J., Butterworth, P. J., & Ellis, P. R. (2014). A novel method for classifying starch digestion by modelling the amylolysis of plant foods using first-order enzyme kinetic principles. *Food & Function, 5*(11), 2751-2758.

Englyst, H. N., Kingman, S. M., & Cummings, J. H. (1992). Classification and measurement of nutritionally important starch fractions. *European Journal of Clinical Nutrition, 46 Suppl 2*(Suppl 2), S33.

Garcia, M. C., Pereira-Da-Silva, M. A., Taboga, S., & Franco, C. M. (2016). Structural characterization of complexes prepared with glycerol monoestearate and maize starches with different amylose contents. *Carbohydrate Polymers, 148*(5), 371-379.

Gary D. Brayer, Gary Sidhu, Robert Maurus, Edwin H. Rydberg, Curtis Braun, Yili Wang, Nham T. Nguyen, Christopher M. Overall, & Stephen G. Withers. (2000). Subsite Mapping of the Human Pancreatic α-Amylase Active Site through Structural, Kinetic, and Mutagenesis Techniques. *Biochemistry, 39*(16), 4778-4791.

Gelders, G. G., Duyck, J. P., Goesaert, H., & Delcour, J. A. (2005). Enzyme and acid resistance of amylose-lipid complexes differing in amylose chain length, lipid and complexation temperature. *Carbohydrate Polymers, 60*(3), 379-389.

Goderis, B., Putseys, J. A., Gommes, C. J., Bosmans, G. M., & Delcour, J. A. (2014). The Structure and Thermal Stability of Amylose–Lipid Complexes: A Case Study on Amylose–Glycerol Monostearate. *Crystal Growth & Design, 14*(14), 3221–3233.

He, J., Liu, J., & Zhang, G. (2008). Slowly digestible waxy maize starch prepared by octenyl succinic anhydride esterification and heat-moisture treatment: glycemic response and mechanism. *Biomacromolecules, 9*(1), 175-184.

Jo, A. R., Kim, H. R., Choi, S. J., Lee, J. S., Chung, M. N., Han, S. K., Park, C. S., & Moon, T. W. (2016). Preparation of slowly digestible sweet potato Daeyumi starch by dual enzyme modification. *Carbohydrate Polymers, 143*(5), 164-171.

Karkalas, J., Ma, S., Morrison, W. R., & Pethrick, R. A. (1995). Some factors determining the thermal properties of amylose inclusion complexes with fatty acids. *Carbohydrate Research, 268*(2), 233-247.

Kawai, K., Takato, S., Sasaki, T., & Kajiwara, K. (2012). Complex formation, thermal properties, and in-vitro digestibility of gelatinized potato starch–fatty acid mixtures. *Food Hydrocolloids, 27*(1), 228-234.

Man, J., Lin, L., Wang, Z., Wang, Y., Liu, Q., & Wei, C. (2014). Different Structures of Heterogeneous Starch Granules from High-Amylose Rice. *Journal of Agricultural & Food Chemistry, 62*(46), 11254-11263.

Meng, S., Ma, Y., Sun, D. W., Wang, L., & Liu, T. (2014). Properties of starch-palmitic acid complexes prepared by high pressure homogenization. *Journal of Cereal Science, 59*(1), 25-32.

Miao, M., Jiang, B., Cui, S. W., Zhang, T., & Jin, Z. (2015). Slowly Digestible Starch-A Review. *Critical Reviews in Food Science & Nutrition, 55*(12), 1642-1657.

Nugent, A. P. (2005). Health properties of resistant starch. *Nutrition Bulletin, 30*(1), 27-54.

Peng, S. L., Xue, L., Leng, X., Yang R. B., Zhang, G., & Hamaker, B. R. (2015). Slow digestion property of octenyl succinic anhydride modified waxy maize starch in the presence of tea polyphenols. *Journal of Agricultural & Food Chemistry, 63*(10), 2820-2829.

Putseys, J. A., Derde, L. J., Lamberts, L., Ostman, E., Björck, I. M., & Delcour, J. A. (2010). Functionality of short chain amylose-lipid complexes in starch-water systems and their impact on in vitro starch degradation. *Journal of Agricultural & Food Chemistry, 58*(3), 1939-1945.

Putseys, J. A., Lamberts, L., & Delcour, J. A. (2010). Amylose-inclusion complexes: formation, identity and physico-chemical properties. *Journal of Cereal Science, 51*(3), 238-247.

Qiao, D., Yu, L., Liu, H., Zou, W., Xie, F., Simon, G., Petinakis, E., Shen, Z., & Chen, L. (2016). Insights into the hierarchical structure and digestion rate of

alkali-modulated starches with different amylose contents. *Carbohydrate Polymers, 144*, 271-281.

Rai, S., Wahile, A., Mukherjee, K., Saha, B. P., & Mukherjee, P. K. (2006). Antioxidant activity of Nelumbo nucifera (sacred lotus) seeds. *Journal of Ethnopharmacology, 104*(3), 322-327.

Stolt, M., Oinonen, S., & Autio, K. (2000). Effect of high pressure on the physical properties of barley starch. *Innovative Food Science & Emerging Technologies, 1*(3), 167-175.

Tian, Y., Li, D., Zhao, J., Xu, X., & Jin, Z. (2014). Effect of high hydrostatic pressure (HHP) on slowly digestible properties of rice starches. *Food chemistry, 152*(2), 225-229.

Tufvesson, F., Wahlgren, M., & Eliasson, A. C. (2003). Formation of Amylose-Lipid Complexes and Effects of Temperature Treatment. Part 2. Fatty Acids. *Starch - Stärke, 55*(3-4), 138–149.

Villay, A., Filippis, F., Picton, L., Cerf, D., Vital, C., & Michaud, P. (2012). Comparison of polysaccharide degradations by dynamic high-pressure homogenization. *Food Hydrocolloids, 27*(2), 278-286.

Wang, S., Wang, J., Yu, J., & Wang, S. (2016). Effect of fatty acids on functional properties of normal wheat and waxy wheat starches: A structural basis. *Food Chemistry, 190*, 285-292.

Xu, H., & Zhang, G. (2014). Slow Digestion Property of Microencapsulated Normal Corn Starch. *Journal of Cereal Science, 60*(1), 99-104.

Zeng, S., Chen, B., Zeng, H., Guo, Z., Lu, X., Zhang, Y., & Zheng, B. (2016). Effect of microwave irradiation on the physicochemical and digestive properties of lotus seed starch. *J Agric Food Chem, 64*(12), 2442-2449.

Zhang, B., Dhital, S., & Gidley, M. J. (2013). Synergistic and antagonistic effects of α-Amylase and amyloglucosidase on starch digestion. *Biomacromolecules, 14*(6), 1945-1954.

Zhang, B., Huang, Q., Luo, F., & Fu, X. (2012). Structural characterizations and digestibility of debranched high-amylose maize starch complexed with lauric acid. *Food Hydrocolloids, 28*(1), 174-181.

Zhang, B., Li, X., Liu, J., Xie, F., & Chen, L. (2013). Supramolecular structure of A- and B-type granules of wheat starch. *Food Hydrocolloids, 31*(1), 68-73.

Zhang, G., Ao, Z., & Hamaker, B. R. (2006). Slow digestion property of native cereal starches. *Biomacromolecules, 7*(11), 3252-3258.

Zhang, G., & Hamaker, B. R. (2009). Slowly digestible starch: concept, mechanism, and proposed extended glycemic index. *Crit Rev Food Sci Nutr, 49*(10), 852-867.

Zhang, Y., Zeng, H., Wang, Y., Zeng, S., & Zheng, B. (2014). Structural characteristics and crystalline properties of lotus seed resistant starch and its prebiotic effects. *Food chemistry, 155*, 311-318.

Zhu, F. (2017). Structures, properties, and applications of lotus starches. *Food Hydrocolloids, 63*, 332-348.

Figure 1

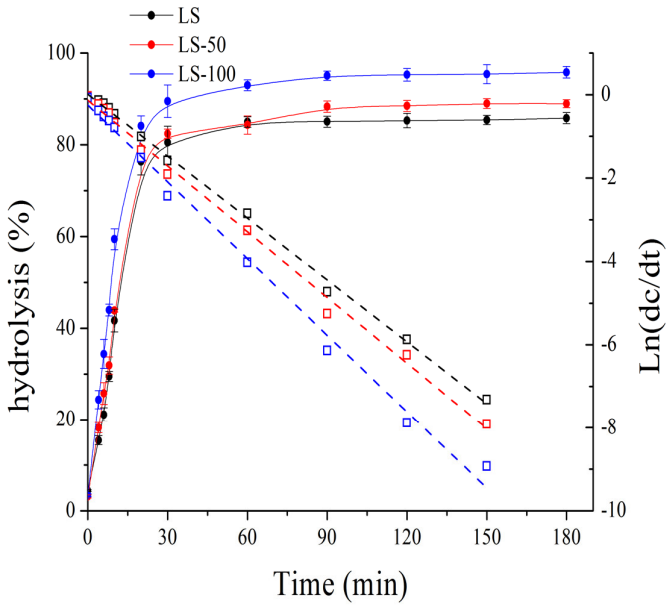

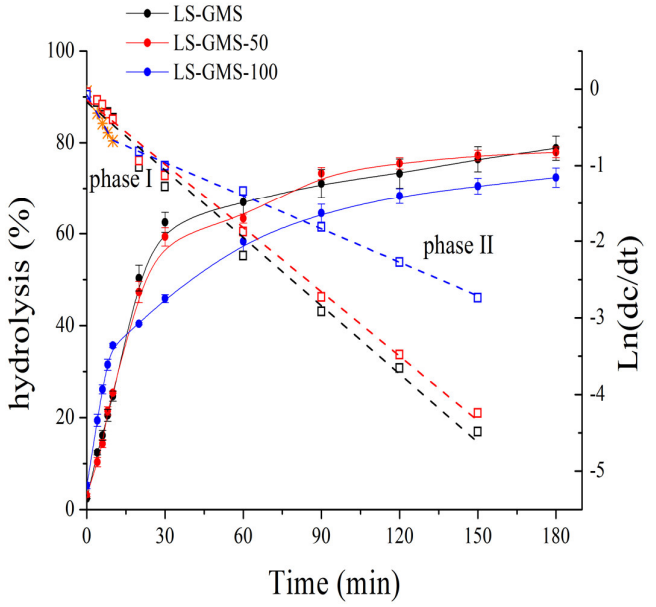

Figure 2

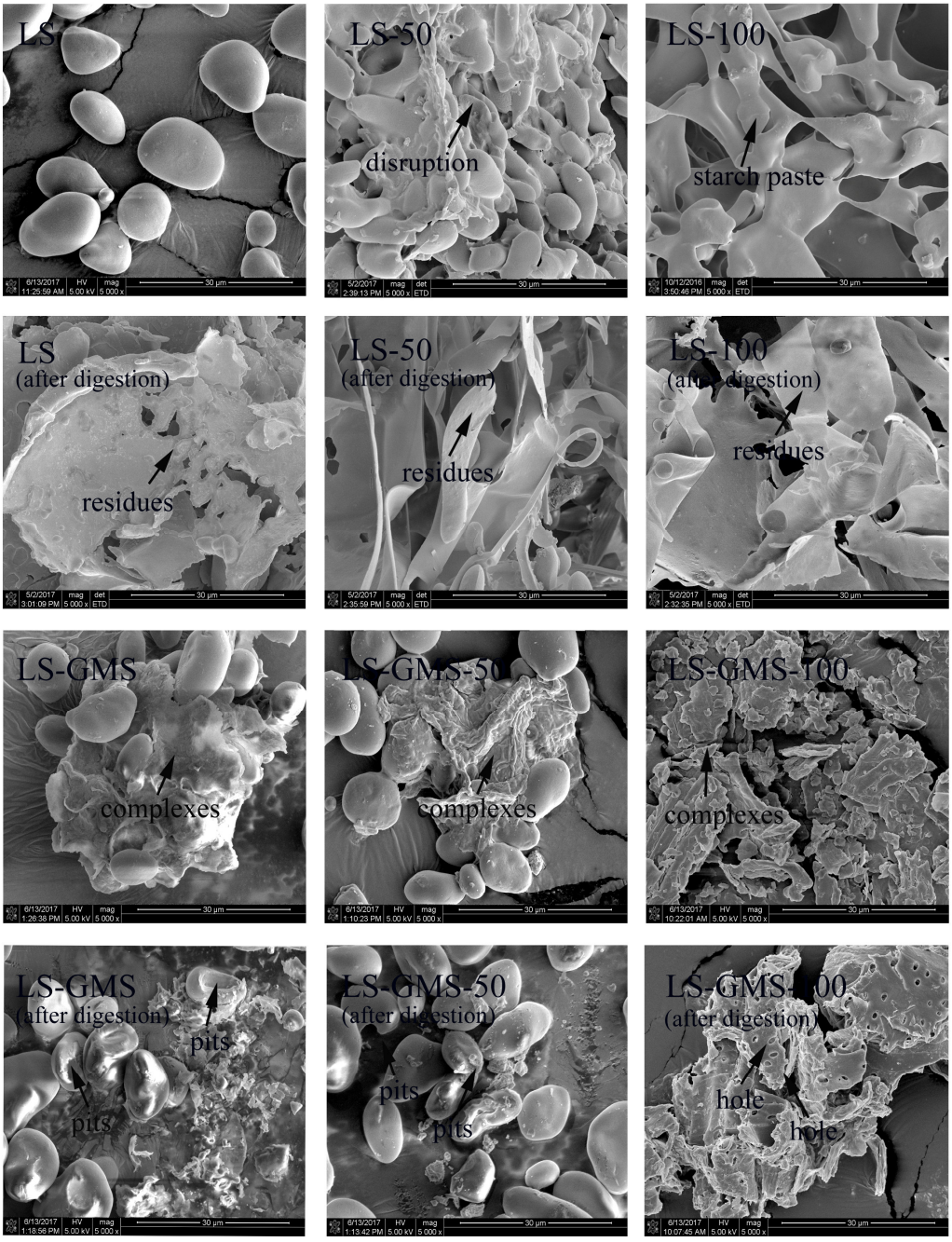

Figure 3

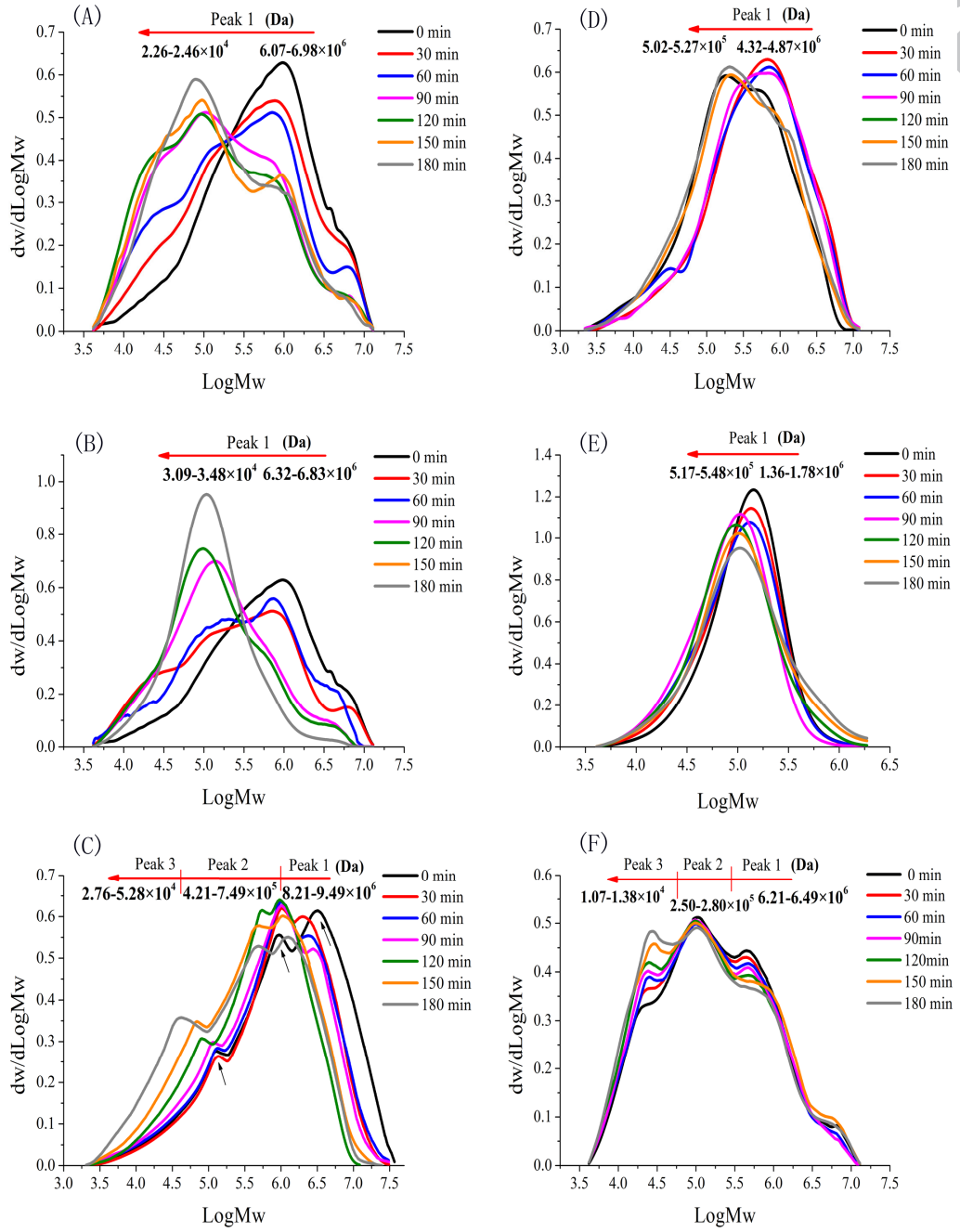

Figure 4

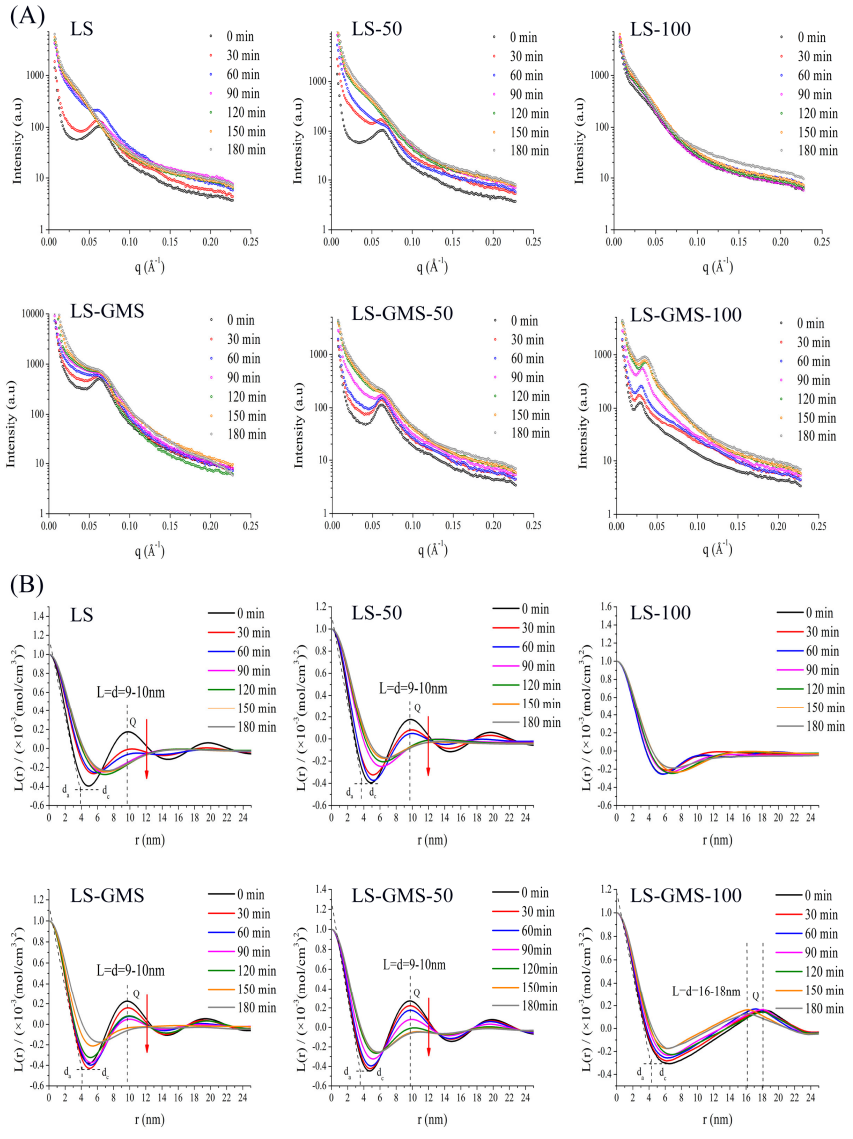

Figure 5

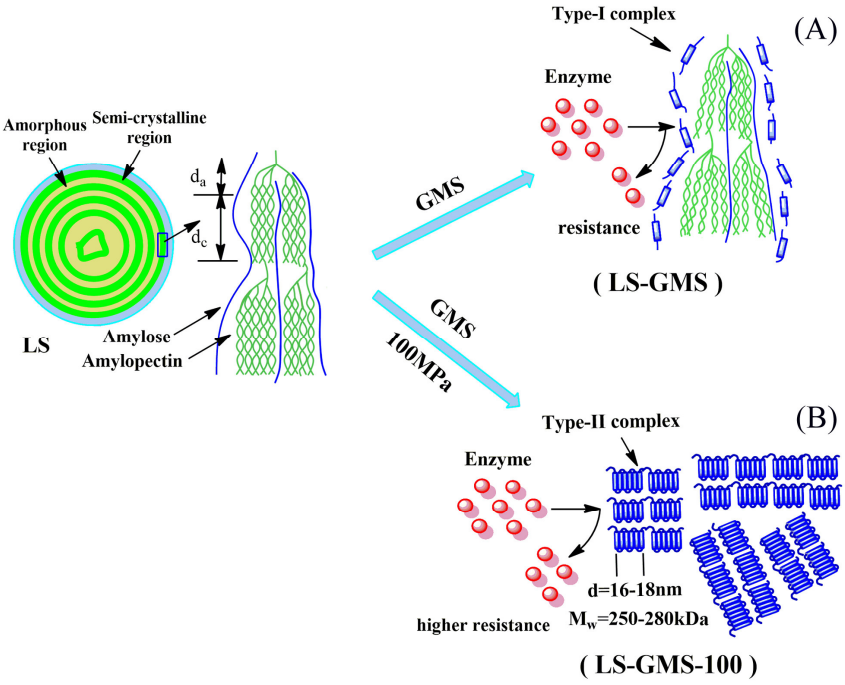

Figure Caption

Figure 1. The digestion curves, LOS plots and fit curves of LS and LS-GMS treated by different homogenization pressures. ○, Experiment data; * and┐ □ , LOS plot data.

Figure 2. The morphology before and after digestion of LS and LS-GMS treated by different homogenization pressures. SEM (5000×)

Figure 3. The molecule weight distribution in digestion of LS and LS-GMS treated by different homogenization pressures. (A) LS; (B) LS-50; (C) LS-100; (D) LS-GMS; (E) LS-GMS-50; (F) LS-GMS-100.

Figure 4. The SAXS patterns (A) and linear correlation function (B) in digestion of LS and LS-GMS treated by different homogenization pressures.

Figure 5. The schematic representation for the difference in slowly digestion process of LS-GMS (A) and LS-GMS-100 (B).

Table 1 The digestive parameters and thermodynamic parameters of LS and LS-GMS prepared by different homogenization pressures.

(A) The digestive parameters of LS and LS-GMS prepared by different homogenization pressure

	D_0	D_{180}	k ($\times 10^{-2}$)		R^2	RDS (%)	SDS (%)	RS (%)
			Phase I	Phase II				
LS	4.39±0.08^{a}	85.79±1.34^{c}	4.42±0.11^{c}	-	0.993	76.65±1.07^{b}	8.64±1.45^{d}	14.21±2.32^{c}
LS-50	3.13±0.12^{b}	89.32±2.32^{b}	4.99±0.07^{b}	-	0.996	78.14±1.87^{b}	9.18±0.87^{d}	12.68±1.38^{c}
LS-100	3.39±0.14^{c}	95.79±1.38^{a}	6.13±0.15^{a}	-	0.992	86.39±2.31^{a}	7.86±0.37^{d}	5.75±0.65^{d}
LS-GMS	2.39±0.12^{d}	79.36±1.37^{d}	2.75±0.06^{e}	-	0.995	53.17±1.98^{c}	23.05±1.67^{c}	23.78±0.34^{b}
LS-GMS-50	3.12±0.11^{d}	77.85±1.66^{d}	2.96±0.10^{d}	-	0.995	50.34±1.76^{d}	25.51±1.13^{b}	24.15±1.13^{b}
LS-GMS-100	5.21±0.13^{e}	74.38±1.87^{e}	6.07±0.15^{a}	1.42±0.06	0.995	39.17±1.45^{e}	33.21±1.32^{a}	27.62±1.53^{a}

Experimental data are the means of duplicates. Values followed by the same superscript letter within a column do not differ significantly ($P < 0.05$).

D_0, the percentage of starch digested at time t=0 (min); D_{180}, the percentage of starch digested at time t=180 (min); k, the starch digestion rate coefficient.

(B) The change of thermodynamic properties of LS and LS-GMS during digestion

		Digestion time (min)						
		0	30	60	90	120	150	180
LS	T_o (℃)	72.24±0.04^{a}	70.39±0.03^{b}	69.13±0.04^{c}	68.93±0.02^{c}	–	–	–
	ΔH (J/g)	2.54±0.10^{a}	1.17±0.05^{b}	0.71±0.13^{c}	0.34±0.08^{d}	–	–	–
LS-50	T_o (℃)	71.32±0.08^{a}	70.04±0.04^{b}	68.29±0.09^{c}	68.21±0.10^{c}	–	–	–
	ΔH (J/g)	2.49±0.10^{a}	0.83±0.10^{b}	0.57±0.10^{c}	0.29±0.08^{d}	–	–	–
LS-100	T_o (℃)	68.67±0.03^{a}	68.06±0.04^{b}	67.69±0.03^{c}	–	–	–	–
	ΔH (J/g)	0.82±0.07^{a}	0.63±0.08^{b}	0.24±0.10^{c}	–	–	–	–
LS-GMS	T_o (℃)	87.86±0.40^{a}	87.43±0.09^{a}	87.22±0.06^{a}	86.32±0.10^{b}	86.21±0.13^{b}	85.31±0.07^{c}	85.28±0.05c
	ΔH (J/g)	2.81±0.10^{a}	2.52±0.10^{b}	2.36±0.07^{c}	2.09±0.11^{d}	1.81±0.07^{e}	1.53±0.03^{f}	1.38±0.06^{g}
LS-GMS-50	T_o (℃)	86.21±0.03^{a}	86.18±0.05^{a}	85.23±0.05^{b}	85.25±0.06^{b}	85.17±0.07^{b}	84.67±0.20^{c}	84.31±0.10^{d}
	ΔH (J/g)	2.85±0.06^{a}	2.68±0.03^{b}	2.26±0.09^{c}	2.14±0.06^{c}	1.98±0.18^{d}	1.62±0.05^{e}	1.52±0.07^{e}
LS-GMS-100	T_o (℃)	108.34±0.21^{a}	108.12±0.13^{a}	108.19±0.06^{a}	107.32±0.11^{b}	106.36±0.15^{c}	106.37±0.24^{c}	110.15±0.25^{d}
	ΔH (J/g)	3.54±0.03^{a}	3.44±0.06^{ab}	3.34±0.04^{bc}	3.32±0.04^{c}	3.26±0.10^{cd}	3.23±0.10^{cd}	3.18±0.06^{d}

Experimental data are the means of duplicates. Values followed by the same superscript letter within a line do not differ significantly ($P < 0.05$). To, onset temperature; ΔH, enthalpy of LS-GMS complexes melting endoderm; "–" means not detected.

Highlight

- HPH treatment decreased the digestive rate of LS-GMS.
- High homogenized pressure (100MPa) changed the molecule and lamellar structure of LS-GMS.
- A strong enzyme-resistance lamellar structure was observed in LS-GMS-100.
- LS-GMS-100 was determined as a type-II complexes.
- The slowly digestible mechanism between LS-GMS and LS-GMS-100 is different.